Bonding and structural changes in siderite at high pressure

GABRIELA FARFAN,[1,*] SHIBING WANG,[1,2] HONGWEI MA,[1,†] RAZVAN CARACAS,[3] AND WENDY L. MAO[1,4]

[1]Geological and Environmental Sciences, Stanford University, Stanford, California 94305, U.S.A.
[2]SSRL, SLAC National Accelerator Laboratory, Menlo Park, California 94025, U.S.A.
[3]CNRS, Ecole Normale Superieure de Lyon, Laboratoire de Sciences de la Terre, Lyon 69342, France
[4]Photon Science, SLAC National Accelerator Laboratory, Menlo Park, California 94025, U.S.A.

ABSTRACT

Understanding the physical and chemical properties of carbonate minerals at extreme conditions is important for modeling the deep carbon cycle, because they represent likely hosts for carbon in the lower mantle. Previous high-pressure studies have identified a structural and electronic phase transition in siderite using X-ray diffraction and X-ray emission spectroscopy. The Fe end-member of the carbonate group, siderite ($FeCO_3$), exhibits unique high-pressure behavior that we investigated using a combination of in situ Raman spectroscopy, synchrotron X-ray diffraction, and theoretical methods. In this Raman spectroscopy study, we observed the appearance of a new CO_3 symmetric stretching mode at 20 cm^{-1} lower frequency beginning at approximately 46 GPa. This softening is due to the lengthening of the C-O bonds as a result of a combination of rotation and volume shrinkage of the FeO_6 octahedra while siderite undergoes the isostructural volume collapse and electronic spin transition.

Keywords: High pressure, diamond-anvil cell, Raman spectroscopy, deep carbon cycle, siderite

INTRODUCTION

Understanding the deep carbon cycle is an area of active research that is critical for modeling the global carbon cycle (Dasgupta and Hirschmann 2010; Hirschmann 2006). If they remain stable at the conditions within the Earth's lower mantle, carbonate minerals may represent an important host for carbon in our planet's deep interior. Previous studies have suggested magnesite ($MgCO_3$) could be an important carbon-bearing compound (Dasgupta and Hirschmann 2010; Fiquet et al. 2002; Isshiki et al. 2004). It undergoes several phase transitions upon compression to over 200 GPa, but does not dissociate into other chemical species (Isshiki et al. 2004; Skorodumova et al. 2005). Siderite ($FeCO_3$) is another potential carbon host that forms a solid solution with magnesite and has been studied to lower mantle pressures (Lavina et al. 2009, 2010a; Mattila et al. 2007; Nagai et al. 2010; Santillán and Williams 2004). Also, recent laser heating experiments on $(Mg,Fe)CO_3$ indicate that at very high pressure and temperature, these carbonates may transform from threefold- to fourfold-coordinated carbon (Boulard et al. 2011).

Previous results on siderite using single-crystal and powder X-ray diffraction (XRD) (Lavina et al. 2009, 2010a; Nagai et al. 2010), X-ray emission spectroscopy (XES) (Mattila et al. 2007), infrared spectroscopy (IR) (Santillán and Williams 2004), and theoretical calculations (Shi et al. 2008) indicate that a series of electronic and structural transitions occur at high pressure (Lavina et al. 2009, 2010a; Nagai et al. 2010). At approximately

50 GPa there is an electronic spin transition associated with an abrupt isostructural volume collapse of ~10% (Lavina et al. 2009).

In this study, we measured the Raman spectra of a natural siderite sample compressed to 50 GPa in a diamond-anvil cell at room temperature. We observed a new symmetric CO_3^{2-} stretching mode (ν_1) emerging at 46 GPa, a pressure that coincides with the electronic spin transition. Our synchrotron XRD results confirm that siderite undergoes an isostructural volume collapse at approximately the same pressure. In addition, state of the art theoretical calculations accurately reproduced the experimentally observed transition pressure and the magnitude of the volume reduction.

METHODS

Experimental methods

As a member of the carbonate group, siderite adopts the space group $R\bar{3}c$ structure at ambient conditions. It can be considered as distorted rock salt structure with Fe^{2+} as the cation and CO_3^{2-} groups as the anions (Lavina et al. 2010). Our starting material was a natural siderite sample from Germany. From electron microprobe analysis we determined the composition to be $(Fe_{0.76}Mn_{0.15}Mg_{0.09}Ca_{0.01})CO_3$, with an uncertainty of approximately 1% in the cation concentrations. Raman spectroscopy is a powerful tool for probing the vibrational modes and can be coupled with a diamond-anvil cell to provide insight into changes in the bonding in carbonates (Shahar et al. 2005). The Raman spectra for the carbonate group have been systematically studied at ambient conditions and different characteristics modes were identified (Rutt and Nicola 1974). For our high-pressure Raman spectroscopy studies, a small single-crystal chip of siderite was loaded into a 120 μm diameter sample chamber drilled into a stainless steel gasket that was compressed inside a symmetric diamond-anvil cell (DAC) with 300 μm diameter flat culets. We used silicone oil as the pressure-transmitting medium and loaded ruby chips for pressure calibration (Mao et al. 1986). A Renishaw RM1000 Raman microscope in the Extreme Environments Laboratory at Stanford University was used to collect

Raman spectra. This system uses a 514 nm laser excitation line and has 4 cm⁻¹ spectral resolution and 2 μm spatial resolution. We also conducted angle-dispersive X-ray diffraction (XRD) at beamline 12.2.2 (λ = 0.4959Å) of the Advanced Light Source (ALS), Lawrence Berkeley National Laboratory (LBNL), and at beamline 16IDB (λ = 0.402965Å) at the Advanced Photon Source (APS), Argonne National Laboratory (ANL), on a siderite sample that we crushed into a powder and loaded with no pressure medium into a symmetric DAC, 300 μm diameter flat culets. All of our experiments were performed at room temperature.

Theoretical methods

To complement our experimental measurements we conducted first-principles calculations on the $FeCO_3$ siderite end-member. We used the planar augmented wavefunctions (PAW) formalism (Blochl 1994) of density functional theory in the ABINIT implementation (Gonze et al. 2009; Torrent et al. 2008). We employed the Perdew-Burke-Ernzerhof (Perdew et al. 1996) flavor of the generalized gradient approximation (GGA) for the exchange correlation portion. The electron density is sampled in reciprocal space using a $6 \times 6 \times 6$ grid of special $\mathbf{k}$-points (Monkhorst and Pack 1976). The kinetic energy cut-offs are 36 Ha for the grid inside and 15 Ha for the grid outside the PAW spheres (1Ha = 27.2116 eV). We considered antiferromagnetic spin configurations and allowed the spin to freely vary during the structural relaxation.

RESULTS AND DISCUSSION

Raman spectroscopy

We observed two modes in siderite above 200 cm⁻¹ (the lower cutoff frequency for our Raman system): the internal symmetric stretching mode (A_{1g}) of the carbonate group denoted ν_1 located at 1088 cm⁻¹, and one of the external E_g modes denoted ν_2 located at 299 cm⁻¹. Our high-pressure Raman spectra indicate that the frequency of ν_1 increases monotonically up to 46 GPa, at which point a new, lower frequency peak appeared (approximately 20 cm⁻¹ lower in frequency that would correspond to the frequency at 30 GPa) (Figs. 1 and 2). The intensity of this new peak increased with pressure at the expense of the original, higher frequency one. The frequency dependence on pressure also decreased above 46 GPa. The dν_1/dP for ν_1 with increasing pressure up to 46 GPa is 2.20 cm⁻¹/GPa. After the phase transition, dν_1/dP of the new peak plateaus or possibly even becomes slightly negative (Fig. 2). The frequency of the external E_g mode also increased with pressure with a dν_2/dP of 3.74 cm⁻¹/GPa, but its intensity diminished until finally disappearing by 35 GPa (Fig. 3). During decompression, the new, lower frequency ν_1 peak disappeared at approximately 42 GPa and the ν_2 peak reappeared at approximately 17 GPa.

Spin transition

Previous high-pressure studies on siderite have reported a pressure-induced, isostructural high-spin (HS) to low-spin (LS) transition due to the increase in the crystal field splitting energy of the 3d electrons of Fe^{2+} in its octahedrally coordinated site under compression. Comparison of these previous studies (Table 1) finds that there is a ~13 GPa range over which the spin transition was observed to take place, might be attributed both to experimental differences and variations in the natural siderite sample composition. Examination of the compositions of the siderite samples shows no obvious correlation between the amount of $FeCO_3$ and the spin transition pressure unlike other lower mantle phases like magnesiowüstite (Mg,Fe)O, which shows a clear increase in transition pressure with increasing FeO content (e.g., Fei et al. 2007). The presence of both peaks likely indicates a coexistence of the LS and HS states and a first-order
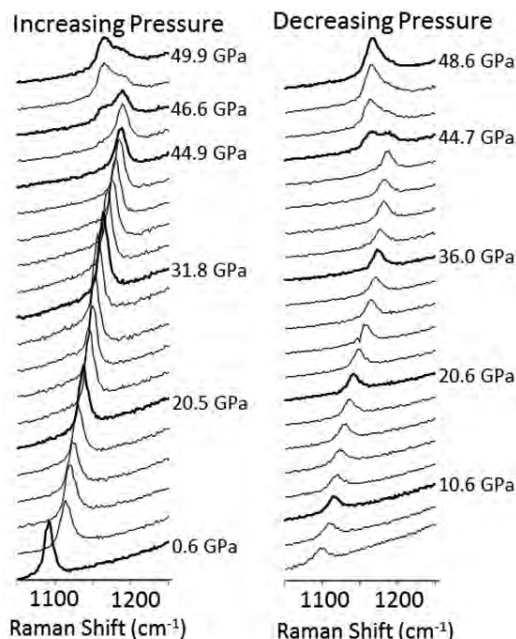

FIGURE 1. Raman spectra for the ν_1 symmetric internal stretching mode (A_{1g}) in the trigonal carbonate group upon compression (**left**) and decompression (**right**). A new lower frequency peak appears at approximately 46 GPa with increasing pressure and disappears at 44 GPa with releasing pressure.
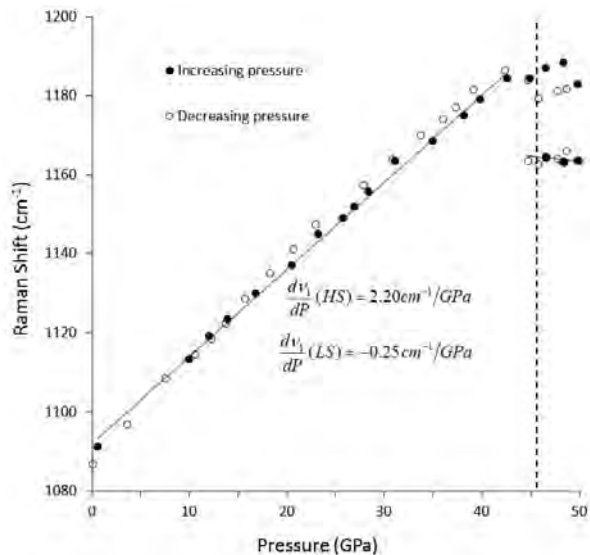

FIGURE 2. Frequency of the ν_1 stretching mode vs. pressure. Data from the increasing pressure cycle is represented by the filled circles and from the releasing pressure by the open circles. Dashed vertical line indicates the appearance of the new peak, which indicates the onset of the spin and structural transition. The data uncertainties fall within the size of the markers.
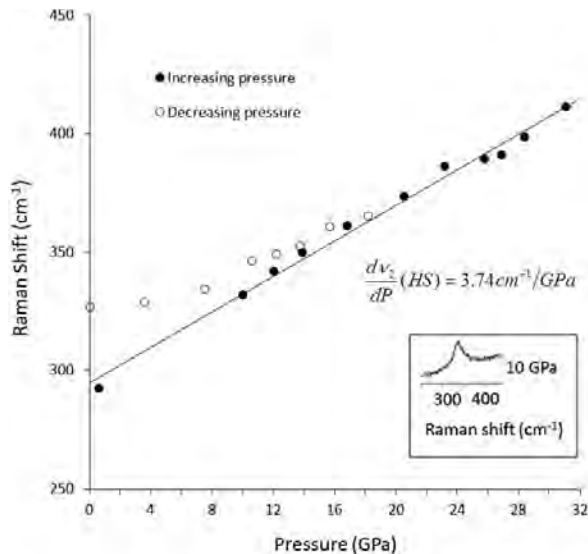
FIGURE 3. Frequency of the E_g external vibration mode (ν_2) vs. pressure upon increasing pressure (filled circles) and decreasing pressure (open circles). Inset: representative spectrum showing the ν_2 peak. The intensity for this mode was quite weak and gradually disappeared at approximately 35 GPa during compression and reappeared below 20 GPa during decompression. The data uncertainties fall within the size of the markers.

TABLE 1. Evolution of lattice parameters for siderite with pressure

P (GPa)	a (Å)	c (Å)	V (Å³)
0.4(1)	4.70(1)	15.41(1)	295.28(2)
5.6(3)	4.67(1)	15.06(1)	282.75(2)
11.4(2)	4.63(3)	14.72(2)	273.61(5)
15.6(2)	4.61(5)	14.50(2)	266.8(5)
19.5(3)	4.60(3)	14.29(6)	261.2(3)
25.5(1)	4.58(2)	14.01(4)	254.1(2)
30.5(1)	4.55(5)	13.79(3)	247.6(5)
35.0(6)	4.54(6)	13.62(3)	243.5(6)
39.8(4)	4.53(4)	13.48(5)	239.6(4)
44.8(1)	4.52(8)	13.33(9)	235.9(8)
50.5(4)	4.52(4)	13.18(6)	232.6(4)
55.2(3)	4.40(5)	12.71(6)	213.4(4)
60.0(4)	4.37(4)	12.48(7)	206.8(4)

Notes: Uncertainties are in parentheses.

phase transition, occurring at approximately 46 GPa when the second peak first appears (Fig. 1). From XRD we see that the transition can be sluggish, taking until 52 GPa to completely transform to the LS state.

X-ray diffraction

We collected XRD data up to just above 60 GPa (Table 1), and the results were consistent with the equation of state from Lavina et al. (2010b) although they trend to slightly higher volume that may be due to the fact that we did not have a pressure-transmitting medium (Fig. 4). From the XRD data, the volume collapse occurred at approximately 52 GPa, which is ~8 GPa higher pressure than the Lavina et al. (2010b) study that used Ne as a pressure medium and 4–6 GPa higher pressure than our Raman spectroscopy results that used silicone oil. With increasing pressure, the Fe^{2+} HS-LS transition occurred, and the LS structure

formed and micro-strains developed in the sample as a result of lattice mismatch between the HS and LS structures. Micro-strains usually do not change peak positions but do broaden the peaks, so micro-strain development can be monitored by the full-width at half maximum (FWHM) of the diffraction peaks. As shown in the pressure vs. FWHM plot for the (012), (104), (110), (113), and (202) reflections, we cannot see exactly where the electronic spin transition begins because the fraction of LS Fe^{2+} and hence the amount of micro-strain and peak broadening are small at the beginning of the transformation (Fig. 5). We do see a sharp increase of the FWHM for all five diffraction peaks at ~45 GPa, likely indicating a significant amount of the HS Fe^{2+} was transforming to LS Fe^{2+} at this pressure, and thus generated a lot of micro-strains as reflected by the peak width. Above 52 GPa, the peaks become sharp again, which can be attributed to the strain release after the spin transition is complete. We can therefore conclude that most of HS Fe^{2+} started to transform to LS at ~45 GPa, and the transformation was complete at ~52 GPa where we see a volume collapse. Visually, Lavina et al. (2009) observed a color change in their sample from clear to green at 50 GPa and green to red 70 GPa. We observed a similar color change to moss green after the spin transition pressure.

Theoretical results

Our XRD results are also in good agreement with our theoretical calculations (Fig. 4). Previous theoretical work found a spin transition in the antiferromagnetic configuration, but seems to underestimate the transition pressure at 15 GPa (GGA) and 28 GPa (GGA+U) (Shi et al. 2008), most likely because of the choice of exchange-correlation formalism (Perdew and Wang 1992). Our enthalpy difference calculations indicate that the low-spin state has lower enthalpy than the high-spin state at approximately 44 GPa. We further observe a loss of magnetization
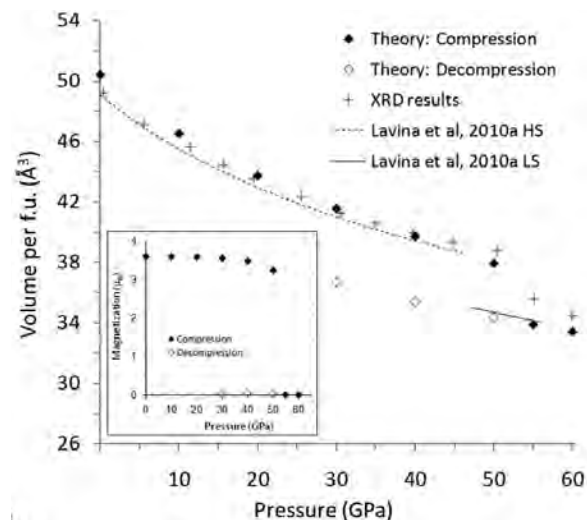

FIGURE 4. Our XRD data (crosses) and theoretical results (open and filled diamonds). The uncertainties for the volumes are smaller than the symbol size. Dotted line is the EOS of high-spin siderite and solid line is the EOS for low-spin siderite (Lavina et al. 2010a). Inset shows calculations of the magnetization with increasing and decreasing pressure.

(Fig. 4, inset) and a volume collapse at high pressures above 50 GPa associated with spin-pairing. Upon decompression, significant hysteresis in the transition was observed in the calculations, as the magnetization and volume collapse were not recovered, even down to 30 GPa (Fig. 4).

Volume collapse and C-O bond lengthening

Lavina et al. (2009, 2010a) reported an ~10% volume collapse associated with the siderite spin transition with an octahedral
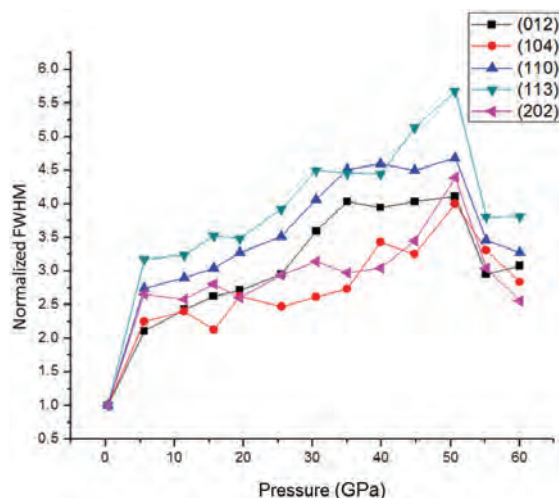

Figure 5. Full-width at half maximum (FWHM) for five of the siderite diffraction peaks. Uncertainties in the normalized FWHM are approximately 0.15. (Color online.)
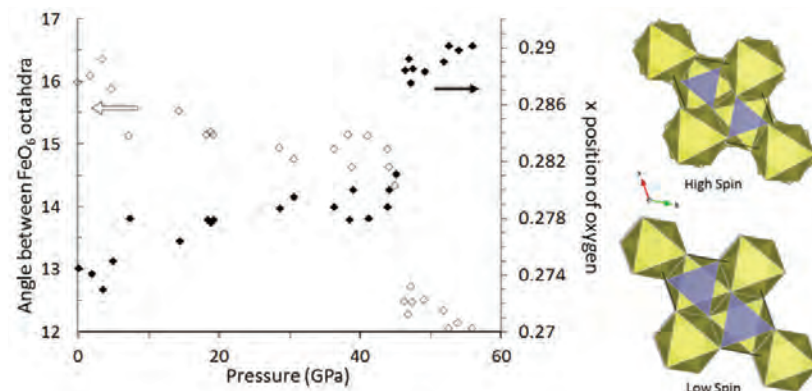
bond distance shrinkage of 4%. Nagai et al. (2010) saw a 6.5% volume collapse and suggested that higher MgO content may reduce the volume collapse at the spin transition due to a lower Fe-content that leads to fewer cations, which undergo the spin transition and volume collapse. Indeed, we observed an ~8% volume collapse in our sample, which is larger than the slightly less Fe-rich sample used by Nagai et al. (2010) and smaller than the very iron-rich sample used by Lavina et al. (2010a) (Table 2). However, for two siderite crystals with different Fe-contents studied by Lavina et al. (2009, 2010a), the reported volume collapse was the same, approximately 10%. This may indicate that for the very Fe-rich samples, the effect of increasing Fe-content on volume collapse is less pronounced. This volume collapse is in excellent agreement with the first-principles calculations.

Our observation of a new lower frequency ν_1 peak with Raman spectroscopy is consistent with a discontinuous increase in the C-O bond length of the carbonate ions that occur at the transition. This expansion is a result of the volume collapse of the FeO_6 group during the high-spin to low-spin Fe^{2+} transition, which, as it contracts, pulls the shared O atoms from the carbonate group causing it to expand and the vibrational modes to "soften" (Fig. 6). This latter behavior is characteristic for molecular-like structures, where covalent building blocks show an expansion during compression, accommodated by the reduction of the inter-block space (e.g., Caracas and Hemley 2007). The change in $d\nu_1/dP$ before and after the spin transition from 2.20 to –0.17 cm^{-1} GPa, respectively confirms this interpretation, which is also consistent with measurements of the C-O bond distance with pressure (Lavina et al. 2010). Lavina's study shows the C-O bond distance decreases (~0.03 Å) linearly up to 45 GPa, consistent with the positive $d\nu_1/dP$ we measured to 46 GPa. After the spin transition

Figure 6. (**left**) Angle between FeO_6 octahedra (filled diamonds) and the x position of the O atoms in the FeO_6 octahedra (open diamonds) with increasing pressure calculated from Lavina et al. (2010a). (**right**) Schematic showing change in structure due to oxygen rotation and FeO_6 octahedra shrinkage (the rotation and shrinkage effects have been exaggerated to make it more obvious to the eye). (Color online.)

TABLE 2. Comparison of previous high pressure studies on Fe-bearing carbonates

	Technique	Sample locale	Composition	Transition pressure (GPa)	ΔV (%) at the transition
Lavina et al. (2009)	Single-crystal XRD	Pribram, Czech Republic	$Fe_{0.72}Mg_{0.24}Mn_{0.03}Ca_{0.01}CO_3$	43	10
Lavina et al. (2010a)	Single-crystal XRD	Ivigtut, Greenland	~$Fe_{0.96}Mg_{0.04}CO_3$	44–45	10
Lavina et al. (2010b)	Single-crystal XRD	Tyrol, Australia	$Mg_{0.87}Fe_{0.12}Ca_{0.01}CO_3$	49–52	–
Mattila et al. (2007)	XES	Ivigtut, Greenland	~$Fe_{0.96}Mg_{0.04}CO_3$	46–56, ~50	–
Nagai et al. (2010)	Powder XRD	unknown	$Fe_{0.73}Mn_{0.22}Mg_{0.05}CO_3$	47–50	6.5
Santillán and Williams (2003)	IR	Estacada, Oregon	$Fe_{0.82}Mg_{0.09}Ca_{0.09}CO_3$	No transition observed to 50 GPa	–
Shi et al. (2008)	Theory	–	$FeCO_3$	15 (GGA), 28(+U=5 eV)	12.5 (GGA),9.7 (+U=5 eV)
This work	Raman and XRD	Germany	$Fe_{0.76}Mn_{0.15}Mg_{0.09}Ca_{0.01}CO_3$	46	8 (XRD)
	Theory	–	$FeCO_3$	52	10

they saw a slight bond lengthening, which can be correlated to the negative $d\nu_1/dP$ we observed above 46 GPa. In magnesite, the C-O bond length was found to decrease from 0–30 GPa, slightly lengthen between 30–50 GPa, and then sharply decrease above 50 GPa using infrared spectroscopy (Santillán et al. 2005). Fiquet et al. (2002) had similar qualitative results for magnesite, but found larger amounts of bond lengthening using angle-dispersive X-ray powder diffraction to 80 GPa. Raman spectroscopy studies on magnesite are currently limited to 32 GPa (Gillet 1993), so it would be interesting to extend these measurements to higher pressure. Santillán et al. (2005) attributed the bond lengthening to rotation of the MgO_6 octahedra. Lavina et al. (2010) observed a similar rotation of the FeO_6 octahedra, which along with the collapse of the FeO_6 due to the spin transition would lengthen the C-O bond (Fig. 6).

Comparison to other carbonates

Although the Ca, Mg, Fe, and Mn carbonate group minerals all have the same structure at ambient conditions, their high-pressure behavior is markedly different. Calcite transforms into an aragonite phase at approximately 2 GPa, a post-aragonite phase at 40 GPa, and a space group $C222_1$ phase over 130 GPa (Ono et al. 2005; Oganov et al. 2008; Santillán and Williams 2004). Magnesite undergoes a phase transition to a pyroxene structure at 113 GPa and later to a $CaTiO_3$-calcite structure at 200 GPa observed experimentally by Isshiki et al. (2004) and in first-principles calculations by Skorodumova et al. (2005). Thus, it remains stable over the pressure range that we are testing with the siderite. Rhodochrosite is stable to at least 50 GPa when pressure is slowly increased, and undergoes an orthorhombic phase transition with a 5% volume collapse when pressure and temperature were rapidly increased (Ono 2007; Santillán and Williams 2004). Ono (2007) estimates the phase transition to occur at ~50 GPa at high temperature with X-ray diffraction.

Concluding remarks

Understanding the phase transitions and high-pressure behavior of common calcite structured carbonates, such as siderite ($FeCO_3$), magnesite ($MgCO_3$), calcite ($CaCO_3$), and rhodochrosite ($MnCO_3$), is critical for modeling how carbon may be stored and cycled in the deep mantle. The presence of a $3d$ transition metal element in siderite leads to the possibility of electronic transitions at conditions existing in the lower mantle, which, in this case, is associated with an isostructural transition and volume collapse. Our Raman spectroscopy, XRD, and theoretical results were consistent with previous studies in terms of transition pressure, amount of volume collapse, and transition pressure hysteresis. Our Raman data revealed a new, lower frequency ν_1 vibrational mode growing above 46 GPa at the expense of the original ν_1 mode, which is a result of the lengthening of the C-O bonds in the carbonate group as the FeO_6 octahedron suddenly shrink and rotate. Comparison with high-pressure studies on other carbonate minerals indicates contrasting behavior (e.g., calcite has a phase transition to aragonite at low pressures, magnesite has a phase transition to the pyroxene structure at 113 GPa, and rhodochrosite has not thus far been shown to undergo spin-transition). In the deep mantle the carbonate composition is likely to be a mixture of many end-members, so the effect of the addition of iron-bearing siderite may need to be considered when considering deep carbon reservoirs and for interpreting seismic observations.

References cited

Blochl, P.E. (1994) Projector augmented-wave method. Physical Review B, 50, 17953–17979.
Boulard, E., Fiquet, G., Guyot, F., Gloter, A., and Perillat, J.P. (2011) A new host for carbon in the deep Earth. Proceedings of National Academy of Sciences, 108, 5184–5187.
Caracas, R. and Hemley, R.J. (2007) New structures of dense nitrogen: Pathways to the polymeric phase. Chemical Physical Letters, 442, 65–70.
Dasgupta, R. and Hirschmann, M.M. (2010) The deep carbon cycle and melting in Earth's interior. Earth and Planetary Science Letters, 298, 1–13.
Fei, Y., Zhang, L., Corgne, A., Watson, H., Ricolleau, A., Meng, Y., and Prakapenka, V. (2007) Spin transition and equations of state of (Mg, Fe)O solid solutions, Geophysical Research Letters, 34, L17307, doi:10.1029/2007GL030712.
Fiquet, G., Guyot, F., Kunz, M., Matas, J., Andrault, D., and Hanfland, M. (2002) Structural refinements of magnesite at very high pressure. American Mineralogist, 87, 1261–1265.
Gillet, P. (1993) Stability of magnesite (MgCO₃) at mantle pressure and temperature conditions: A Raman spectroscopic study. American Mineralogist, 78, 1328–1331.
Gonze, X., Amadon, B., Anglade, P.M., Beuken, J.M., Bottin, F., Boulanger, P., Bruneval, F., Caliste, D., Caracas, R., Côté, M. and others. (2009) ABINIT: First-principles approach to material and nanosystem properties. Computer Physics Communications, 180, 2582–2615.
Hirschmann, M.M. (2006) Water, melting, and the deep earth H₂O cycle. Annual Review of Earth and Planetary Sciences, 34, 629–653.
Isshiki, M., Irifune, T., Hirose, K., Ono, S., Ohishi, Y., Watanuki, T., and others. (2004) Stability of magnesite and its high-pressure form in the lowermost mantle. Nature, 427, 60–63.
Lavina, B., Dera, P., Downs, R.T., Prakapenka, V., Rivers, M., Sutton, S., and Nicol, M. (2009) Siderite at lower mantle conditions and the effects of the pressure-induced spin-pairing transition. Geophysical Research Letters, 36, L23306.
Lavina, B., Dera, P., Downs, R.T., Tschauner, O., Yang, W., Shebanova, O., and Shen, G. (2010a) Effect of dilution on the spin pairing transition in rhombohedral carbonates. High Pressure Research, 30, 224–229.
Lavina, B., Dera, P., Downs, R.T., Yang, W., Sinogeikin, S., Meng, Y., Shen, G., and Schiferl, D. (2010b) Structure of siderite FeCO₃ to 56 GPa and hysteresis of its spin-pairing transition. Physical Review B, 82, 064110.
Mao, H.K., Xu, J., and Bell, P.M. (1986) Calibration of the ruby pressure gauge to 800 kbar under quasi-hydrostatic conditions. Journal of Geophysical Research, 91, 4673–4676.
Mattila, A., Pylkkänen, T., Rueff, J.P., Huotari, S., Vankó, G., Hanfland, M., Lehtinen, M., and Hämäläinen, K. (2007) Pressure induced magnetic transition in siderite FeCO₃ studied by X-ray emission spectroscopy. Journal of Physics: Condensed Matter, 19, 386206.
Monkhorst, H.J. and Pack, J.D. (1976) Special points for Brillouin-zone integrations. Physical Review B, 13, 5188–5192.
Nagai, T., Ishido, T., Seto, Y., Nishio-Hamane, D., Sata, N., and Fujino, K. (2010) Pressure-induced spin transition in FeCO₃-siderite studied by X-ray diffraction measurements. Journal of Physics: Conference Series, 215, 012002.
Oganov, A.R., Ono, S., Ma, Y., Glass, C.W., and Garcia, A. (2008) Novel high-pressure structures of MgCO₃, CaCO₃ and CO₂ and their role in earth's lower mantle. Earth and Planetary Science Letters, 273, 38–47.
Ono, S. (2007) High-pressure phase transformation in MnCO₃: A synchrotron XRD study. Mineralogical Magazine, 71, 105–111.
Ono, S., Kikegawa, T., Ohishi, Y., and Tsuchiya, J. (2005) Post-aragonite phase transformation in CaCO₃ at 40 GPa. American Mineralogist, 90, 667–671.
Perdew, J.P. and Wang, Y. (1992) Accurate and simple analytic representation of the electron-gas correlation energy. Physical Review B, 45, 13244.
Perdew, J.P., Burke, K., and Ernzerhof, M. (1996) Generalized gradient approximation made simple, Physical Review Letters, 77, 3865–3868.
Rutt, H.N. and Nicola, J.H. (1974) Raman spectra of carbonates of calcite structure.

Journal of Physics C: Solid State Physics, 7, 4522.

Santillán, J. and Williams, Q. (2004) A high-pressure infrared and X-ray study of $FeCO_3$ and $MnCO_3$: Comparison with $CaMg(CO_3)_2$-dolomite. Physics of the Earth and Planetary Interiors, 143–144, 291–304.

Santillán, J., Catalli, K., and Williams, Q. (2005) An infrared study of carbon-oxygen bonding in magnesite to 60 GPa. American Mineralogist, 90, 1669–1673.

Shahar, A., Bassett, W.A., Mao, H.K., Chou, I-m., and Mao, W.L. (2005) The stability and Raman spectra of ikaite, $CaCO_3 \cdot 6H_2O$, at high pressure and temperature. American Mineralogist, 90, 1835–1939.

Shi, H., Luo, W., Johansson, B., and Ahuja, R. (2008) First-principles calculations of the electronic structure and pressure-induced magnetic transition in siderite $FeCO_3$. Physical Review B, 78, 155119.

Skorodumova, N.V., Belonoshko, A.B., Huang, L., Ahuja, R., and Johansson, B. (2005) Stability of the $MgCO_3$ structures under lower mantle conditions. American Mineralogist, 90, 1008–1011.

Torrent, M., Jollet, F., Bottin, F., Zerah, G., Gonze, X., (2008) Implementation of the projector augmented-wave method in the ABINIT code: application to the study of iron under pressure. Computational Materials Science, 42, 337–351.